Computational Prediction of Stall Flutter in Cascaded Airfoils

F. Sisto,* S. Thangam,† and A. Abdel-Rahim‡
Stevens Institute of Technology, Hoboken, New Jersey 07030

At off-design conditions turbomachines may experience flow separation from the cascaded airfoils and the circumferential pattern of stalled and unstalled airfoils propagates about the flow annulus. The unsteady periodic nature of propagating stall will force blade vibration; stall flutter of the blades may occur if stall synchronization occurs and the propagation frequency is entrained by the blade natural frequency. In this study a computational scheme based on a modified form of the vortex method is used to simulate the flow over an infinite linear cascade of airfoils. The structural model is based on a two-dimensional characteristic section with one degree of freedom in either torsion or bending. The aerodynamic loading and the structural displacements are solved simultaneously by a time-marching technique. Results are presented for an airfoil cascade with constant geometry, onset flow, and stall cell wavelength as a function of the reduced frequency. Over an appreciable finite interval of blade frequency, the stall frequency becomes entrained (i.e., departs from the value it would have in the presence of completely rigid blades) and synchronization of the two frequencies occurs. This is the region of stall flutter and the details of entrainment, or synchronization, are studied in detail. Implications concerning future computational studies and the potential impact on design are presented.

Nomenclature

A_b = blade cross-sectional area
c = blade chord
c = blade stiffness coefficient
D = blade damping coefficient
f = frequency
j = complex constant, $\sqrt{-1}$
K = reduced frequency, $\pi fc/U_\infty$
N = number of blades
N_ω = number of vortices in the computational domain
p = stall cell wavelength
s = distance along the airfoil surface
t = time
U_∞ = upstream approach velocity
V = velocity
u,v = velocity components
x,y = coordinates of the airfoil
z = complex coordinate, $x + jy$
α = inlet flow angle
β = cascade stagger angle
Γ = vortex strength
ν = kinematic viscosity
ρ = fluid density
ψ = stream function
ε = bounded support for the vortex blobs
σ = interblade phase angle
Θ = torsional displacement, radi
ω = vorticity
Ω = airfoil angular velocity

Subscripts and superscripts

n = blade normal
s = blade surface
t = torsion

Received March 2, 1990; presented as Paper 90-1116 at the AIAA/ASME/ASCI/AHS/ASC 31st Structures, Structural Dynamics, and Materials Conference, Long Beach CA, April 2–6 1990; revision received March 6, 1991; accepted for publication March 8, 1991.

*George Meade Bond Profesor, Department of Mechanical Engineering. Associate Fellow AIAA.
†Professor, Department of Mechanical Engineering. Member AIAA.
‡Graduate Research Assistant, Department of Mechanical Engineering.

Introduction

STALL flutter in the blading of axial-flow turbomachines has been a persistent operational problem for nearly half a century.[1] The phenomenon is differentiated from the stall flutter of single airfoils by the interblade phasing inherent with multiple airfoils. With a single airfoil the aeroelastic vibration in the pure bending mode has often been termed "buffeting" and has displayed a chaotic content.[2] The highly twisted, inertially coupled turbomachinery blade usually results in an appreciable torsional component even in the so-called predominantly bending mode. As the incidence is increased toward the surge line in an axial compressor, or fan, the interblade phasing manifests itself first as part of an unsteady fluid motion. Stalling is confined to regularly spaced circumferential patches of individual blades while the flow remains unstalled in the intervening spaces. This pattern of stalled flow and interspersed unstalled flow propagates along the annular cascade of airfoils, the so-called "rotating stall," giving rise to a time lag, or phasing, between occurrence of similar events at adjacent airfoils. This is in effect an interblade phase angle.

The phase angle so defined may occur without the benefit of blade vibration. It is clear that the periodic flow variations produce fluctuating aerodynamic reactions, and thus the blades which in fact are not completely rigid, are free to respond structurally to the varying aerodynamic loads. Depending upon the magnitude of these fluctuating loads and the relationship between the blade natural frequency and the loading frequency, the structural response can be either significant or insignificant. At this stage of physical explanation the distinction between forced vibration and self-excited vibration (flutter) is not differentiated. However, when the blade vibration amplitude does become appreciable in some sense, it is not unexpected that the flow will be modified as a result. The physical characteristics of the (steady and unsteady) flow within a cascade of airfoils will depend to a very great extent upon the (steady or unsteady) boundary conditions at the airfoil surfaces. It is this mutual interaction between the fluid and the structure which characterizes aeroelasticity and which leads to the self-excited instability that can be characterized as "cascade stall flutter."

The stall-unstall sequence of a particular blade, although periodic, is highly nonlinear, with the formation of large vortical structures in the flow and sudden changes in the lift and moment acting on each blade. The shedding and convection of vorticity is an essential element of the physical process and

gives rise to the self-excited flow instability. It is for this reason that the vortex method[3] is particularly appropriate for modeling unsteady stalled flow in cascades. In fact, the use of (bound and free) vorticity as the primitive variable for modeling unsteady airfoil reactions has a long history[4] and applies as well to cascades of airfoils.[5]

Formulation and Method of Solution

The physical configuration consists of a linear cascade of staggered, cambered airfoils in high Reynolds number two-dimensional flow (Fig. 1). A reference frame fixed to the cascade is used. Thus the blades are at rest except for possible vibratory motion and the stall cells move past them. The y-axis represents the tangential direction and the x-axis the axial direction. The inflow angle is measured with respect to the axial direction in this frame. The stagger angle and the camber angle are also marked on the sketch. In the following text, a brief description of the formulation and the method of solution will be given.

The vorticity field for two-dimensional, viscous, incompressible flow past an infinite linear cascade of airfoils is governed by the equation

$$\frac{\partial \omega}{\partial t} + u\frac{\partial \omega}{\partial x} + v\frac{\partial \omega}{\partial y} = \nu\left(\frac{\partial^2 \omega}{\partial x^2} + \frac{\partial^2 \omega}{\partial y^2}\right) \tag{1}$$

where

$$\omega = \frac{\partial v}{\partial x} - \frac{\partial u}{\partial y} \tag{2}$$

The vorticity within the airfoil is $\omega = 2\Omega_b$, where Ω_b is the angular velocity in the torsional motion. The boundary condition in terms of the vorticity may be written as

$$\oint \nu\frac{\partial \omega}{\partial n} = -2A_b\left(\frac{\partial \Omega_b}{\partial t} + u\frac{\partial \Omega_b}{\partial x} + v\frac{\partial \Omega_b}{\partial y}\right) \tag{3}$$

It should be noted that the system of equations governing the vorticity and the system of equations governing the velocity and pressure field are equivalent. A stream function ψ can be defined as

$$u = \frac{\partial \psi}{\partial y} \text{ and } v = -\frac{\partial \psi}{\partial x} \tag{4}$$

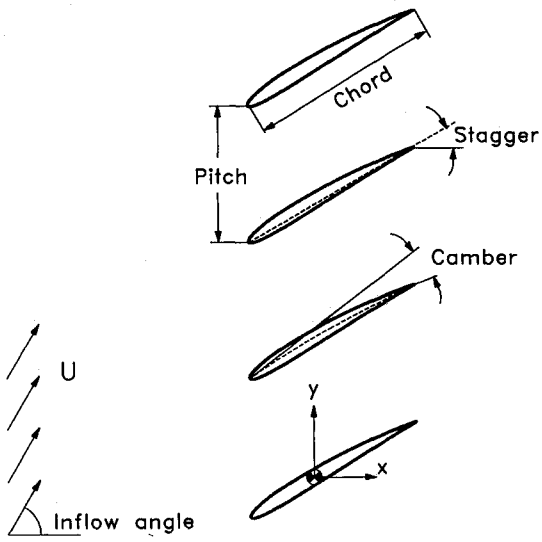

Fig. 1 Schematic of the airfoil cascade.

which satisfies the continuity equation. Combining Eqs. (2) and (4) yields the Poisson equation

$$\nabla^2 \psi = -\omega \tag{5}$$

A vortex method first proposed by Spalart[3] for a stationary cascade was later successfully modified and refined for the analysis of stall propagation in rigid linear cascades by Jonnavithula et al.[6] In addition, the vortex method has recently been shown to yield accurate prediction of the unsteady aerodynamics of cascaded airfoils under nonstall conditions by Sisto et al.[7] In the present study the unsteady areodynamics are analyzed using this method. The cascaded airfoils are modeled structurally as single degree-of-freedom linear oscillators in either bending or torsion. Figure 2 shows the structural dynamics model.

As in physical applications involving axial-flow turbomachinery, these blades are subject to a self-excitation mode. The essence of the present aeroelastic stall-flutter studies is, therefore, the coupling of the unsteady aerodynamics algorithm with the structural dynamics algorithm for simultaneous solution by a time-marching technique. Figure 3a shows the overall flowchart for the computations, with Figs 3b–d showing in more detail the individual flowcharts for aerodynamics, time-marching, and structural dynamics, respectively. At each time step the aerodynamics subprogram receives the position and velocity of each blade in order to satisfy the boundary condition, and the structural program in turn receives the lift and moment along with the position and velocity of each blade to compute its new position and velocity. The stream function can then be used to depict the flowfield and help interpret the result. The vortex method involves the discretization of the computational domain into a large number of finite vortex blobs which convect with the mean flow but do not change their strength, i.e.,

$$\omega = \sum_{k=1}^{N_\omega} \omega_k \tag{6}$$

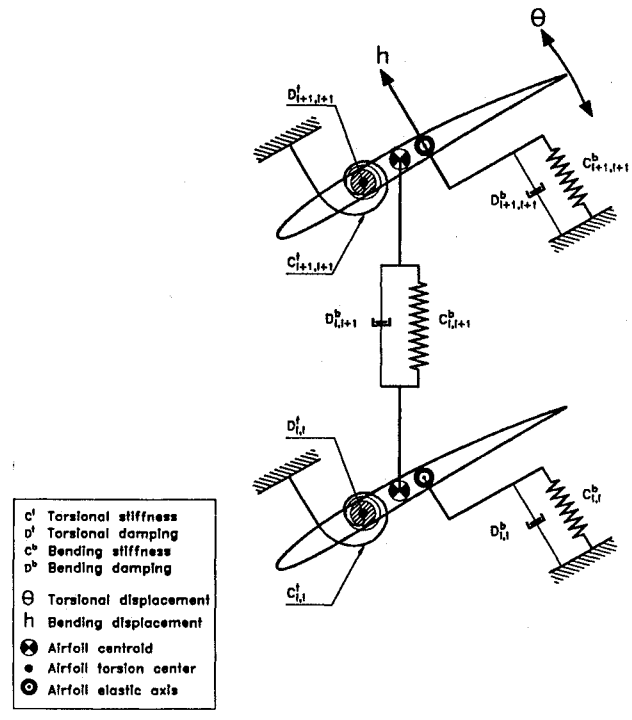

Fig. 2 Schematic of the structural dynamics model.

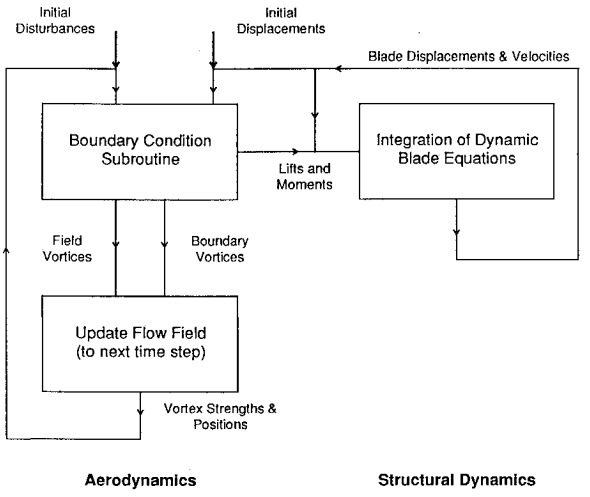

a) Computational sequence and flowchart

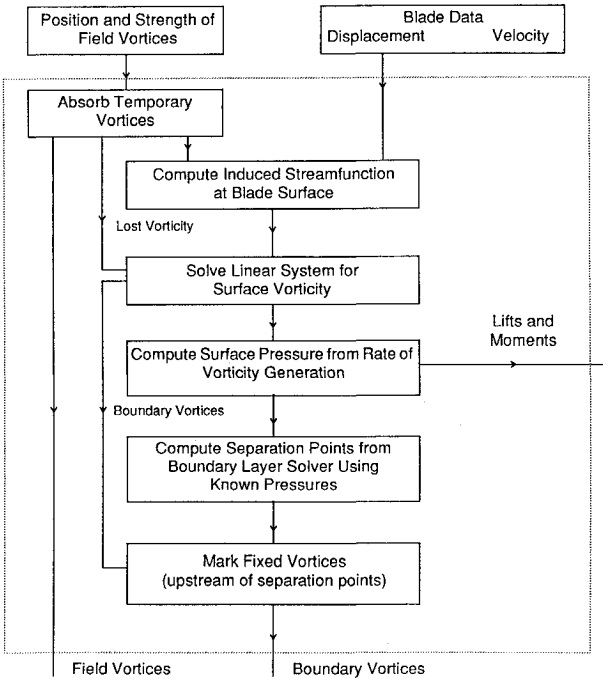

b) Subroutine for aerodynamic boundary conditions

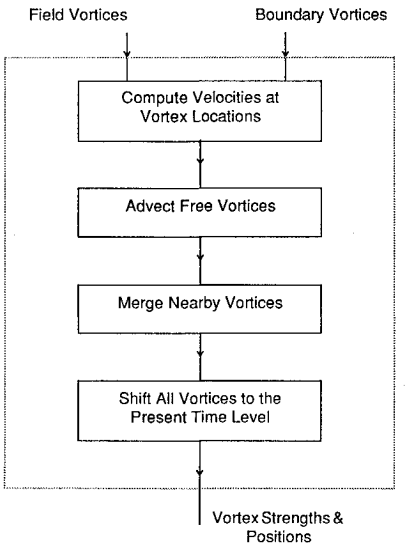

c) Time-marching scheme for the vortex method

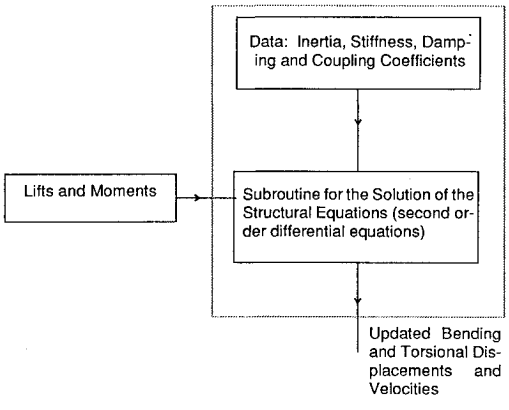

d) Structural dynamics subroutine

Fig. 3 Overall and individual flowcharts.

The corresponding stream function induced by the collection of vortices $\Sigma\psi_k$, where

$$\psi_k = \left(\frac{\Gamma_k}{4\pi}\right) \ln\left\{\left|\sin\left[\frac{2\pi j}{p}(z - z_k)\right]\right|^2 + \varepsilon^2\right\} \qquad (7)$$

is readily determined.[8] The complex variable $z = x + jy$, and p is the period of the array. The parameter ε (which acts as a bounded support for the vortex blobs) smooths out the singularity at $z = z_k$. The upstream boundary condition is set computationally as uniform flow at a prescribed flow angle one chord length upstream of the cascade leading edges. The periodicity condition states that flow variables are repeated identically over any two points separated by N blade pitches where N is a prescribed integer. Satisfaction of the boundary conditions on the blade surfaces determines the vortex strengths everywhere and the induced velocity of the bound and free vortices determines the downstream boundary condition, typically three chord lengths downstream of the trailing edges. For computational purposes the vortex strengths at the downstream boundary are averaged over N pitches and replaced by a single vortex sheet of constant strength. Ideally the periodicity condition should be imposed with N equal to the integer number of blades in the corresponding annular blade row. Stemming from the large computational times involved with such large N, actual values have been restricted to $N = 2$ or 3 in the past.

In practice, the blades of a turbomachine are twisted, tapered, and connected to each other by stiffening rings or shrouds. In order to investigate the flowfield in such a device, a fully three-dimensional model would be required for both the blade structure and the aerodynamics. Owing to both computer limitations as well as due to the limitations of the solution techniques used in this study, the cascade is modeled to be linear and in pure torsional vibration. However, the results obtained should still provide physical insight into this important aeroelastic problem.

The instantaneous coordinates of the airfoil surface under pure torsion are given by

$$z_i(t) = z_i(t_0)\theta^{j\Theta(t)} \tag{8}$$

and the torsional velocities are

$$\dot{z}_i(t) = jz_i(t_0)\dot{\Theta}(t)e^{j\Theta(t)} \tag{9}$$

where $z_i(t_0)$ are the airfoil complex coordinates at the initial time t_0 measured from its centroid, assumed here to coincide with the torsion center, and $\Theta(t)$, $\dot{\Theta}(t)$ are the instantaneous displacement and velocity for torsional vibrations, respectively. At the airfoil surfaces, the nonpenetration condition is imposed, which requires that the normal velocity of the fluid at the body surface equal the normal velocity of the body. From the instantaneous coordinates of the airfoils, the normal vector $\boldsymbol{n}$ at each point can be evaluated at each time step. Since

$$\boldsymbol{V} \cdot \boldsymbol{n} = \boldsymbol{V}_b \cdot \boldsymbol{n} \tag{10}$$

and the relation $\partial_s \psi = v_n$, where n and s are the local coordinates normal and parallel to the wall, respectively, the incremental value of the stream function on the boundary of the airfoil in torsional oscillation can be expressed as

$$\delta\psi|_s = \int_{s_0}^{(s_0+\delta s)} (\boldsymbol{V}_b \cdot \boldsymbol{n})\, ds = \int_{s_0}^{(s_0+\delta s)} v_n\, ds \tag{11}$$

This equation is used to determine the stream function distribution along the boundary points of the blades and thus to form the boundary conditions needed to solve the vorticity stream function equation. As a consequence of the blade motion, the stream function is not constant along the airfoil boundaries. It should also be emphasized that the *no-slip* boundary condition is satisfied in a weak sense. In the physical flow, the vorticity diffused out due to the action of viscosity. To achieve a similar effect the newly created vortices are located a small distance (of about the core size of the vortices) away from the airfoil surface to ensure that they can convect with the flow. Since there are no singularities within the airfoil, the flow there is irrotational with zero circulation and all the circulation is contained in the vortex sheet located outside the airfoil. These conditions have in the past been successfully implemented for both rigid as well as vibrating airfoils.[3,6,7] The analytical model is currently limited by the necessity to impose periodicity (through specification of the parameter p), by the boundary layer routine used to predict separation, and by the assumption of incompressible flow. These limitations may be ameliorated in the future at the expense of computational complexity.

The computational procedure is shown in the form of flowcharts in Figs 3a–d, and additional details may be found in Spalart,[3] Jonnavithula et al,[6] and Sisto et al.[7] All computations reported in this work were performed using a CYBER-205 supercomputer. Fifty boundary points were used to define each solid body, and the number of vortices in the flowfield was kept at five times the total number of boundary points. Thus for a three-blade cascade, 750 vortices were used. A typical computation for a three-blade cascade involved time marching over 8000 steps (of size 0.5 time units) and required approximately 100 min of CPU time.

Results and Discussion

In Fig. 4 the instantaneous streamline patterns are shown at uniform time intervals for a cascade in torsional vibration with a prescribed flow periodicity over three-blade passages (i.e., an average interblade phase angle ($\sigma = 2\pi/3$ or $-2\pi/3$). The cascaded airfoil has 10-deg circular arc camber with NACA 0008 thickness distribution and is set at zero stagger with unit

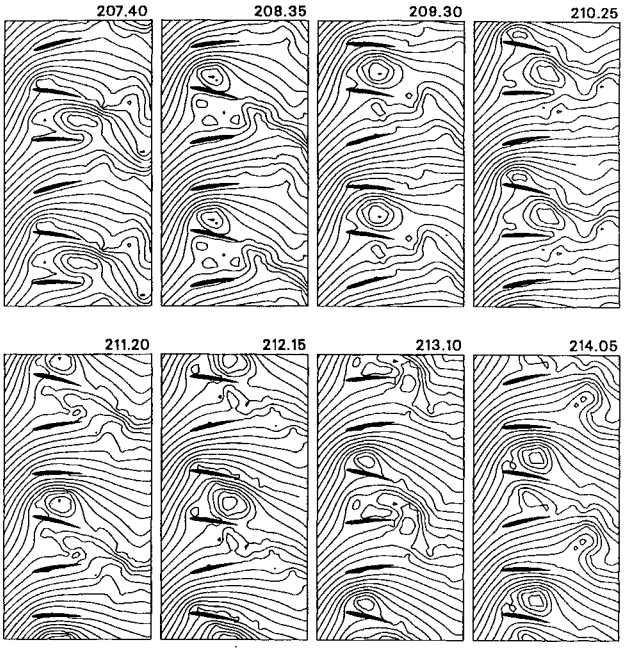

Fig. 4 Instantaneous streamline pattern for a cascade in torsional vibration at different time levels over a single period of oscillation (cascade periodicity is three; stagger = 0 deg, inflow angle = 55 deg, blade natural frequency in vacuum = 0.13 Hz, and the corresponding reduced frequency = 0.408)

solidity. Other flow and structural parameters are described in Fig. 4. Inspection will show a departure from geometric periodicity attributable to the instantaneous blade displacements. In this particular example the large vortical structures and the propagation of the stall patches are apparent.

The frequency of stall at a given blade is near the structural natural frequency. The complete aeroelastic computational model can be considered as an eigenvalue problem in which the stall frequency/stall celerity constitute the characteristic value and the fluid velocity distribution (including circumferential periodicity) and the blade mode constitute the characteristic function. Analysis of Fig. 4 yields the interesting result that in fact for this set of data the interblade phase angle σ selected is $2\pi/3$ and not its negative counterpart. This accords more with practical experience where σ is positive and less than π, corresponding to a so-called backward traveling wave with respect to imputed rotor velocity. The actual interblade angle is established by the computational solution to the problem. For example, with an imposed circumferential periodicity of three-blade passages, an average interblade phase angle of 120 or 240 deg can establish itself. However, any three phase angles summing to 360 deg could appear in the solution (e.g., 115, 110, and 135 deg). It is interesting and important to note that an average of 120 deg seems to be preferred to 240 deg in the cases studied so far. If a periodicity of six-blade passages were to be imposed, the computational solution could conceivably display an average interblade phase angle of 0, 60, 120, 180, 240, or 300 deg, only one of which would be selected. For the sample numerical study the interblade phase angle of the blade vibrations is determined entirely by the aerodynamics, since there is no interblade structural coupling in the model. The same is true of the stall wave celerity, except that within the entrainment interval the celerity is modified by the periodic blade displacements, thus revealing the aeroelastic nature of the synchronization phenomenon, i.e., stall flutter.

At these same conditions the spectrum of the computed torsional displacements is shown in Fig. 5 and the spectrum of the computed aerodynamic moment appears as Fig. 6. It is seen that peaks in both spectra occur at the same (stall and natural) frequencies; the cascade is in torsional stall flutter.

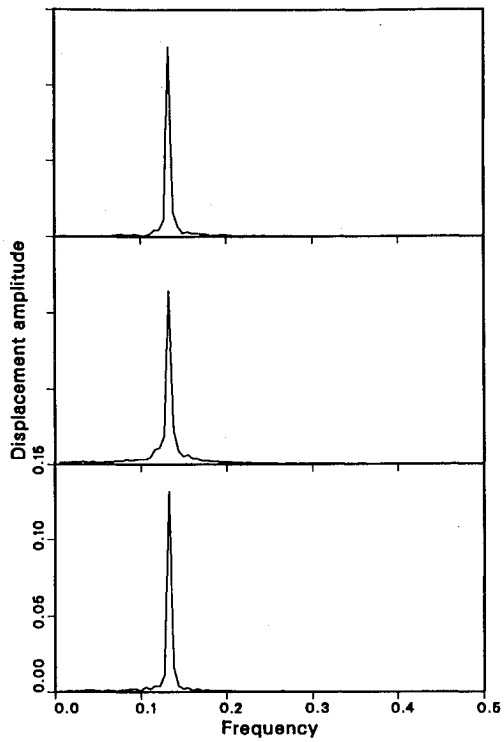

Fig. 5 Displacement spectra for a three-blade cascade in torsional vibration (other details are the same as in Fig. 4).

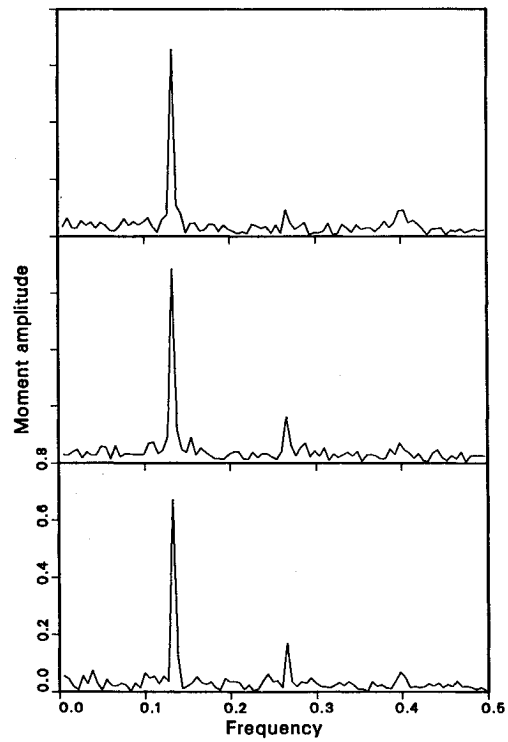

Fig. 6 Aerodynamic moment spectra for a three-blade cascade in torsional vibration (other details are the same as in Fig. 4).

It is the behavior of cascaded airfoils as the stall characteristic frequency approaches the blade frequency that is being intensively examined in the present study. It should be noted that the flutter frequency is virtually identical with the blade natural frequency owing to the large mass ratio of the blade to the fluid. Whereas the displacement is very nearly a pure sinusoid, the moment displays higher harmonics of the fundamental frequency, indicating the nonlinear nature of the periodic fluid response.

The computational investigations have shown that, in the torsional mode under stalling condition, the basically nonlinear phenomenon of frequency entrainment, or synchronization, occurs. The entrainment process is graphically displayed in Fig. 7. This figure has been constructed by maintaining the cascade geometry and onset flow as constants and varying the structural stiffness to produce changes in the reduced frequency of vibration. These structural frequencies are computed by Fourier analysis from the response and are only slightly changed from the frequencies *in vacuo*, which may be computed directly for these simple single-degree-of-freedom models.

When the fundamental stall frequency and the blade natural frequency are well separated, the low-amplitude response of the blade is predominantly at the structural frequency. This is attributable to the small but finite content of the moment at that frequency; the underlying physical aspects of the fluid motion, and the nature of the vortex method as well, each exhibit a small chaotic component across a broad band of frequencies. Within a small band of frequencies as the blade structural frequency approaches the fundamental stall frequency from above or below, the stall frequency is entrained by the blade frequency. Then single large peaks occur with substantial amplitudes of blade displacement and aerodynamic moment at identical frequencies as described above. Torsional stall flutter can be said to occur on the interval of entrainment. The linear structural subsystem has entrained the nonlinear aerodynamic subsystem and the combined system of fluid and structure can be considered to be undergoing self-excitation.

Further insight into the flutter/entrainment phenomenon is contained in Fig. 8 which depicts the oscillatory amplitude of the blade displacement as a function of the blade reduced frequency. It is seen that within the entrainment interval of frequency the amplitude displays a peak value at the coincidence of the blade natural frequency with the "undisturbed" stall frequency. In one sense this could be interpreted as typical resonance behavior as an oscillator is swept by a range of forcing frequencies. However, in the present case the "forcing" frequency is in fact being controlled by the oscillator, again emphasizing the self-excited nature of the response.

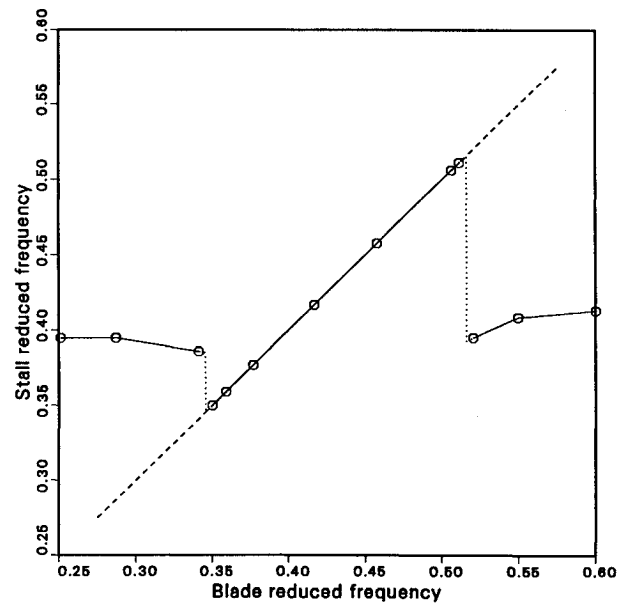

Fig. 7. Influence of blade-reduced frequency on the stall-reduced frequency for a cascade in torsional vibration (other details are the same as in Fig. 4). The plot shows the entrainment of the stall frequency on a certain interval of blade frequency.

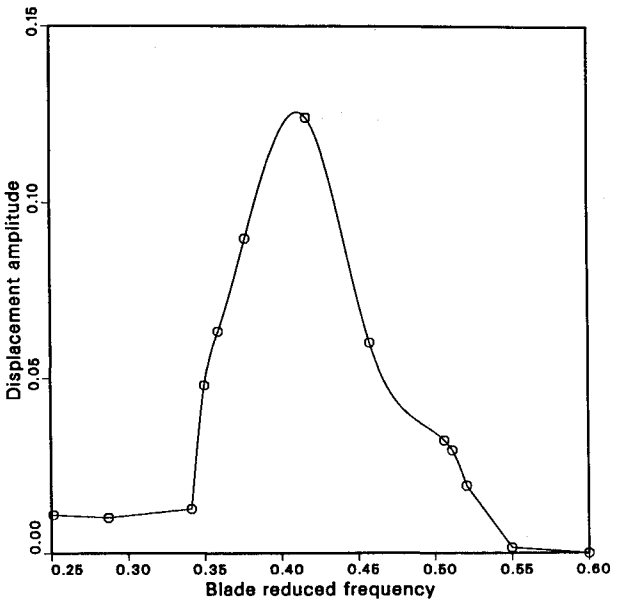

Fig. 8 Influence of blade-reduced frequency on the blade amplitude of a cascade in torsional vibration (other details are the same as in Fig. 4). The plot shows substantial displacement amplitude in the entrainment interval.

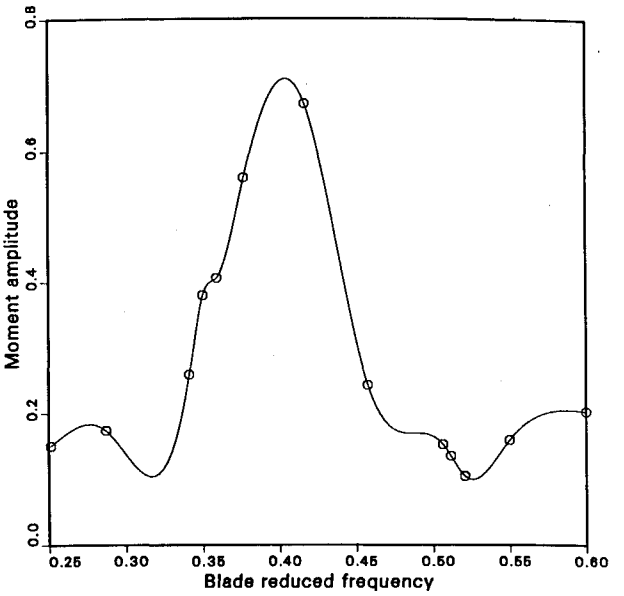

Fig. 9 Influence of blade-reduced frequency on the blade moment amplitude of a cascade in torsional vibration (other details are the same as in Fig. 4). The plot shows the moment amplitude as the fundamental frequency of stall.

Additional insight is provided by the fact that the vibration amplitude builds up to the peak and then decreases as the blade frequency is varied. For linear, or classical flutter, in the absence of mechanical damping no such smooth variation would be obtained; rather, the predicted amplitude would become infinite at the flutter point and would otherwise be null. The present nonlinear behavior explains in part why the stall flutter amplitude grows gradually from zero as the flutter region is transversed along a typical compressor or fan operating line.[1] It should be emphasized, however, that the intersection or coincidence of stall frequency with blade frequency in the turbomachine is attained with near constant, or slowly varying, structural natural frequency as the stall frequency is varied by changing the shaft speed and associated throughflow. The slow changes in structural natural frequency are due to rotational effects and apparent mass effects which respond to the changing shaft speed.

The blade stiffness undoubtedly affects the oscillating blade amplitude for a specific dynamic pressure of the fluid flow. The exact relationship of the parameters that affect blade amplitude has not been sorted out. Material damping (which is neglected in the sample computations) will certainly affect the result. The width of the entrainment interval will also be influenced. It is known that finite intervals of entrainment have been observed in actual compressors that were instrumented to simultaneously measure rotor blade vibratory strain and rotating stall passing frequency. The conventional interpretation is that a "resonance" occurs between the blade structural frequency and the rotating stall frequency, characteristically described as a nonintegral engine order excitation. The appearance of measurable intervals of frequency entrainment indicate that typical blades are sufficiently flexible to exhibit this phenomenon.

Figure 9 provides a measure of the oscillatory moment amplitude inside and outside the entrainment region. The highest values of this moment near the center of the interval give a strong indication that the nonlinear self-excitation process results in the shedding of stronger vortices and the appearance of larger vortical structures within the cascade. These suppositions are borne out by comparing the computed streamline patterns and typical vortex strengths inside and outside the entrainment interval.

As a result of the present computational study there is a better appreciation of the interaction between the periodic flow in the flow annulus of an axial-flow turbomachine and the periodic structure comprised of the multiplicity of identical airfoils in the annular cascade. This periodicity is in the direction of the cascade periphery and its steady-state implications (with a wavelength of one blade pitch) have been well understood. The unsteady manifestation of the flow involving airfoil stall and termed propagating (or rotating) stall has also been understood and the propagation speed, or celerity, of the stall pattern is in general amenable to computation. Although stall flutter of the cascaded blades has been observed, the relationship between periodically stalling flow and the vibration of the blades has not heretofore been accessible to computation. It should be noted here that there is no direct experimental data to validate the computational results. There are some indirect experimental results[6,9] to suggest that the interblade phase angles, σ, are qualitatively correct. A more direct experimental verification would be costly but extremely useful.

The present study has indicated clearly that the flexibility of the airfoil does in fact exert a degree of control over the stall propagation celerity within the entrainment interval of frequencies. When the interblade phase angle (or the number of diametral nodes, or the number of stall patches) remains constant while the stall frequency is changed by entrainment, there must be a corresponding change in the propagation velocity. Thus the rotating stall phenomenon in a completely rigid set of airfoils is not identical in all respects when the blades are endowed with the flexibility of the real structure. Because the magnitude of the frequency interval over which entrainment occurs cannot be expressed analytically, we must resort to computational solutions to explore the extent of control which a given degree of blade flexibility exerts over stall propagation velocity. A parametric study of this problem is required using computational solutions of the highly nonlinear unsteady aerodynamics model aeroelastically coupled to a linear (or weakly nonlinear) structural dynamics model. Direct solutions of the unsteady Navier-Stokes equations may be utilized in place of the vortex method. The latter still requires improvement of the boundary layer algorithm.

Concluding Remarks

The stall propagation/stall flutter mechanism needs to be studied computationally in respect to other aspects of the

phenomenon. Since the aerodynamic moment is a periodic function with higher harmonics evident in the computational results, is entrainment of the stall frequency possible through a near coincidence of its strong second harmonic with the blade frequency? What are the potentialities for subharmonic resonance/entrainment? In particular, preliminary computations seem to indicate that pure bending stall flutter in the conventional range of reduced frequency is different in character from the torsional stall flutter.[9] The extent of this difference and the explanation thereof is being actively pursued. Since the practical manifestation of stall flutter in cascade occurs with a coupled bending-torsion mode, a study of the two-degrees-of-freedom case is mandatory.

More extensive ramifications are related to the role of the interblade phase angle σ. On a rotor, or in an annular cascade, σ is restricted to the values $2\pi n/N$ where n is an integer, N is the number of blades in the row, and $1 \leq n < N$. On a rotor undergoing system vibration, the number of diametral nodes is a surrogate for the interblade phase angle. Thus, two diametral nodes imply $\sigma = \pm 4\pi/N$, three diametral node imply $\sigma = \pm 6\pi/N$, and so on. Rotor system vibration characterized by diametral nodes is said to have forward traveling waves when the interblade phase angle σ has positive values. This is the usual situation in physically observed stall flutter vibrations.[9]

These remarks apply to a perfectly tuned system. With mistuning (either structural or aerodynamic) the requirement on σ becomes simply

$$\sum_{i=1}^{N} \sigma_i = 2\pi n$$

so that blade-to-blade variations are possible but annular geometry recognizes that the Nth blade is at the same time the zeroth blade. It appears from this discussion that the interblade phase angle, or its surrogate, is selected in the physical case (or the numerical simulation) by the relative stability, or ease of entrainment, of different rotating stall patterns. Thus, the studies based on the present method of enforcing periodicity over two-, three-, or four-, etc. blade passages could explain the behavior of a particular rotor (or stator) and the system modes exhibited at flutter. Ultimately, the objective would be to enforce periodicity over N blade passages in order to compute the complete stall flutter mode, in which case the stall wavelength need not encompass an integral number of blade passages, and, in point of fact, the mistuned stage could be fully accommodated. The present supercomputer time requirements for the general solution outlined above are, of course, prohibitive, while the analysis of the full three-dimensional problem is still more demanding.

Acknowledgments

The supercomputer time for this work was provided by the John von Neumann National Supercomputer Center, Princeton, New Jersey and by the NASA Lewis Research Center, Cleveland, Ohio. Acknowledgment is also made to Stevens Institute of Technology for the use of the Institute's computer facilities.

References

[1]Sisto, F. "Stall Flutter," *AGARD Manual on Aeroelasticity in Axial Flow Turbomachines*, Vol. 1, AGARDograph No. 298, 1987, Chap. VII.

[2]Fung, Y. C. *An Introduction to The Theory of Aeroelasticity*, Dover, 1969.

[3]Spalart, P. R. "Two Recent Extensions of the Vortex Method," AIAA Paper 84-0343 (1984).

[4]Theodorsen, T., "General Theory of Aerodynamic Instability and the Mechanism of Flutter," NACA Rept. 496, 1934.

[5]Sisto, F., "Unsteady Aerodynamic Reactions of Airfoils in Cascade," *Journal of Aeronautical Sciences*, Vol. 22, 1955, pp. 297–302.

[6]Jonnavithula, S., Thangam, S., and Sisto, F., "Computational and Experimental Study of Stall Propagation in Axial Compressors," *AIAA Journal*, Vol. 28, 1990, pp. 1945–1952.

[7]Sisto, F., Wu, W., Thangam, S., and Jonnavithula, S., "Computational Aerodynamics of Oscillating Cascades with the Evolution of Stall," *AIAA Journal*, Vol. 27, 1989, pp. 462–471.

[8]Lamb, H., *Hydrodynamics*, Dover, 1945.

[9]Stargardter, H., "Fan Flutter Test," *AGARD Manual on Aeroelasticity in Axial Flow Turbomachines*, Vol. 2, AGARDograph No. 298, 1988, Chap. XX.